Nanochem. Res., 9(1): 19-27, Winter 2024

RESEARCH PAPER

Synthesis of Metal Oxide Nano Particles by Sol-Gel Method and Investigation of its Biomedical Applications

Hajira Tahir[1]*, Muhammad Saad[1], Mehreen Latif [2] , S. Tanweer Hyder[1] and Rameez Ahmed[1]

[1] Department of Chemistry, Karachi University, Pakistan
[2] Department of Biochemistry, Bahria University Medical & Dental College, Karachi, Pakistan

ARTICLE INFO

Article History:
Received 20 Jul 2023
Accepted 05 Dec 2023
Published 01 Jan 2024

Keywords:
Antioxidant,
Enzyme inhibition activities,
Nanocomposites,
Sol gel method,
IC_{50}.

ABSTRACT

In this investigation, CuO NPs, Cu-MnNCs, and Cu-Co NCs were synthesized by the sol gel method in the presence of the stabilizing agent polyvinyl alcohol (PVA). These nanoparticles were characterized by Fourier transform infrared spectroscopy (FTIR), scanning electron microscopy (SEM), and X-ray diffraction (XRD) techniques. The chemical structure and existence of bonding of PVA integration with nanoparticles were verified by the FTIR analysis. The SEM investigations revealed that the average particle sizes of CuO NPs, Cu-Mn NCs, and Cu-Co NCs were 64.5, 87.5, and 69.0 nm, respectively. Additionally, the XRD analysis supported their nano sizing.

The antioxidant and enzyme inhibition activities were assessed against 2, 2-diphenyl-1-picryl-hydrazyl (DPPH) with IC_{50} values of 78.9, 67.8, and 60.8 g/ml, respectively. The antioxidant activities showed that they inhibited the effects of oxidative metabolites.

The IC_{50} value is a quantitative measure that reveals the presence of certain inhibitory chemicals required to block the biological process in vitro .The biological component could be an enzyme, microorganism, or cell receptor. The enzyme inhibition activities of CuO NPs, Cu-Mn NCs, and Cu-Co NCs against urease were found to be 18.5, 23.7, and 34.5 uM, respectively. These characteristic properties suggested that these nanocomposites have biomedical applications. Moreover, they can be efficiently employed for therapeutic purposes.

How to cite this article
Tahir H., Saad M., Latif M., Hyder S. T., Ahmed R., Synthesis of Metal Oxide Nano Particles by Sol-Gel Method and Investigation of its Biomedical Applications. Nanochem. Res., 2024; 9(1): 19-27. DOI: 10.22036/NCR.2024.01.03

INTRODUCTION

Nonomaterials are fascinating class of substances that are highly sought for a range of useful applications. They can have incredibly large surface areas and possess exceptionalmagnetic, electrical, optical, mechanical, and catalytic properties. Their properties manage their sizes, shapes, synthesis circumstances, and appropriate functionalization.

More focus has recently been placed on copper (Cu) and copper-based nanoparticles, notably in the field of catalysis. They also serve as catalysts in gas-phase, photocatalysis, and electrocatalysis processes [1]. Additionally, Cu has several distinct physical and chemical characteristics and is a 3D transition metal.It has a wide range of accessible oxidation states(Cu^0, Cu^I, Cu^{II}, and Cu^{III})and can go through a wide variety of reactions. Numerous applications for the Cu-based nanocatalysts exist in disciplines such as nanotechnology, including electrocatalysis, photocatalysis, and catalytic organic transformations [2-5]. The main challenging issue is the development of catalytic

* Corresponding Author Email: *hajirat@uok.edu.pk*

NPs that are highly active, stable, and affordable.

The anchoring of Cu NPs (such as Cu, CuO, or Cu_2O) on supports such as iron oxides, SiO_2, carbon-based materials, or polymers is one practical method for producing improved Cu-based nanomaterials for catalysis. Additionally, (Cu) has a high boiling point which makes it compatible with high temperature and pressure in chemical processes, including continuous flow reactions, microwave-assisted reactions, vapor-phase reactions, and various organic transformations. Their conducive and catalytic properties have wide applications [6–9].

The excellent antibacterial activity of the CuO NPs and their potential as disinfectants make them a common choice for biological applications. The higher bactericidal capabilities against various Gramm + ve and Gramm - ve bacterial strains are employed in wound dressings and have also shown fungicidal effects [10-12]. They are often employed as biosensors to detect glucose, dopamine, cholesterol, lactate, DNA, and other substances. Furthermore, their prospective significance as antitumor drugs in the treatment of malignancies, such as lung, breast, prostate, and kidney, is a critical issue. They are also utilized as efficient nano carriers [12,13]. In addition, it is essential for cellular respiration, controlling neurotransmitter levels, collagen protein formation, and the metabolism of key elements like iron[14,15].

When creating various nanoparticles chemically, capping agents are used which act as reducing and stabilizing agents. They are often introduced with precursors at the beginning of the process [16]. For instance, in a study, copper sulphate salt was used as a precursor and aniline as a capping agent to create CuO nanoparticles. In various studies, copper acetate was used as a precursor to co-precipitate chitosan and stabilized copper oxide nanoparticles (CuO NPs). They were calcinated at a temperature of 500 °C, resulting in the formation of NPs with a size varying below 35 nm [16,17]. The co-precipitation method was used to synthesize PEG and PVP-capped CuO NPs below 27 nm sized. Ultrasonic vibrations are employed in the sono chemical process to synthesize nanoparticles (NPs). Recently, copper sulphate precursor was employed to synthesize CTAB stabilized CuO NPs[18].

Nanomaterials are synthesized by using a variety of techniques, including chemical, physical, and biological ones. The advantage of the synthesis process is to combine its capacity with nanomaterials and it has various biological applications [19].

The antioxidants, which can be either man-made or natural, can halt or delay specific forms of cell damage by consuming a diet rich in fruits and vegetables. A government policy in the United States encourages individuals to consume more of these items since it has been shown that a diet containing fruits and vegetables is healthful. Studies have not yet shown that antioxidant supplements might prevent diseases. Antioxidant supplements 'potential to prevent illnesses has not yet been demonstrated by trials. Beta-carotene, lutein, lycopene, zeaxanthin, selenium and multivitamins are examples of chemicals that are antioxidants [20].According to research, people who consume more fruits and vegetables are less likely to suffer diseases.

Free radicals are highly reactive molecules that occasionally reduce or oxidize other atoms. Mitochondria are by-products of aerobic respiration's transport system based on electrons and are a major cause of reactive species. Superoxide radicals are generated when 1–3% of the electrons prematurely interact with oxygen, despite the majority of them successfully progressing the third impaired transport chain based on electron [21]. Super and nitric oxides are produced through macrophages and neutrophils, which support phagocytosis and also allow cells to destroy pathogens. This is one of the essential physiological processes made possible by the formation of free radicals. Free radicals can produce lengthy chemical chains in the body because they interact so rapidly with other molecules.

Oxidative stress is caused in the body due to an imbalance between free radicals and antioxidants. It has an impact on cardiovascular diseases[22]. The vascular wall has three important types of cells: smooth muscle cells, endothelial cells, and macrophages, which possess the ability to produce free radicals that have strong contact for peroxidation of lipids. When there is an abnormally high level of oxidized lipids present over time, the high activation rate can harm blood vessels and lead to the development of foam cells and plaque growth, both indicators of atherosclerosis. Additionally, hardness in endothelial cells is due to the LDL oxidizing process, which is also cytotoxic. Antioxidants, including beta-carotene and vitamin E, are crucial for avoiding numerous

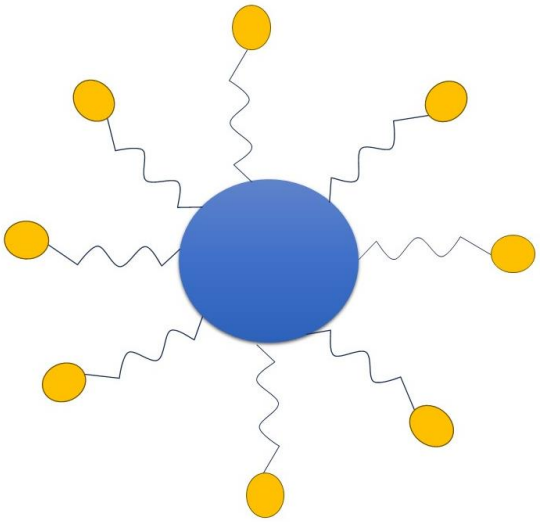

Fig. 1: Representation of Metal oxide Nanoparticles incorporated with PVA

cardiovascular illnesses [23]. Fig. 1 represent Metal oxide nanoparticles with PVA polymer interaction.

The synthetic polymer PVA, which has hydroxyl groups, is also employed as a complex drug carrier. In the most typical method, vinyl acetate (VAc) is polymerized with the aid of free radicals to produce the intermediate polyvinyl acetate (PVAc), which is subsequently hydrolyzed with a strong base while being present in methyl alcohol.The physical and functional characteristics of PVA are ultimately determined by the process parameters and the degree of PVAc hydrolysis, and it may be classified into grades that have either been completely or partially hydrolyzed.

This work aims to find enzyme inhibition activity in the synthesized nanoparticles and they are employed to demonstrate their biomedical applications.

EXPERIMENTAL

MATERIALS AND METHODS

Chemicals and Materials

Common solvents, acids, and bases were purchased in Analar grade from known vendors. PVA (polyvinyl Alcohol),copper chloride tetrahydrate ($CuCl_2.4H_2O$), $MnCl_2.3H_2O$, ferric chloride ($FeCl_3.6H_2O$), and 0.1M of Cobalt Chloride ($CoCl_2.4H_2O$)were purchased from Sigma-Aldrich.

Preparation of PVA

For the preparation of PVA, about 4.0 g of it was dissolved in 100 ml of distillated water and heated for 30 minutes. Additionally, 5 ml of 1M HNO_3 was added in order to dissolve the solution.

Preparation of CuO Nanoparticles

Polyvinyl alcohol (PVA) was combined with 0.1M of copper chloride tetrahydrate ($CuCl_2.4H_2O$) and 0.5M of sodium hydroxide anhydrous pellets of (NaOH) were incorporated. The NaOH was dissolved in deionized distilled water, and the resultant solution was added drop by drop over the course of 30 minutes to an aqueous copper chloride tetrahydrate solution. The solution was sonicated repeatedly until complete precipitation occurred. The powder was air-dried before undergoing room-temperature drying. After that, it was subjected to calcination for 2 hours at temperatures ranging between 400 to 700 °C [24].

Preparation of Cu-Mn Nanocomposite

As the initial precursors, approximately 0.1 M of Copper Chloride Tetrahydrate ($CuCl_2.4H_2O$), 0.5 M of Sodium hydroxide anhydrous pellets (NaOH), and the presence of polyvinyl alcohol (PVA) were utilized. NaOH was dissolved in deionized water, and the resulting solution was added drop wise to a combination of $CuCl_2.4H_2O$ and $MnCl_2.3H_2O$. The solution was repeatedly sonicated until it precipitated. The material was first dried at room temperature, followed by calcinations for 2 hours at 700 °C [25].

Preparation of Cu-Co Nanocomposite

Cobalt chloride ($CoCl_2.4H_2O$) and ferric chloride ($FeCl_3.6H_2O$) were dissolved in 100 ml of

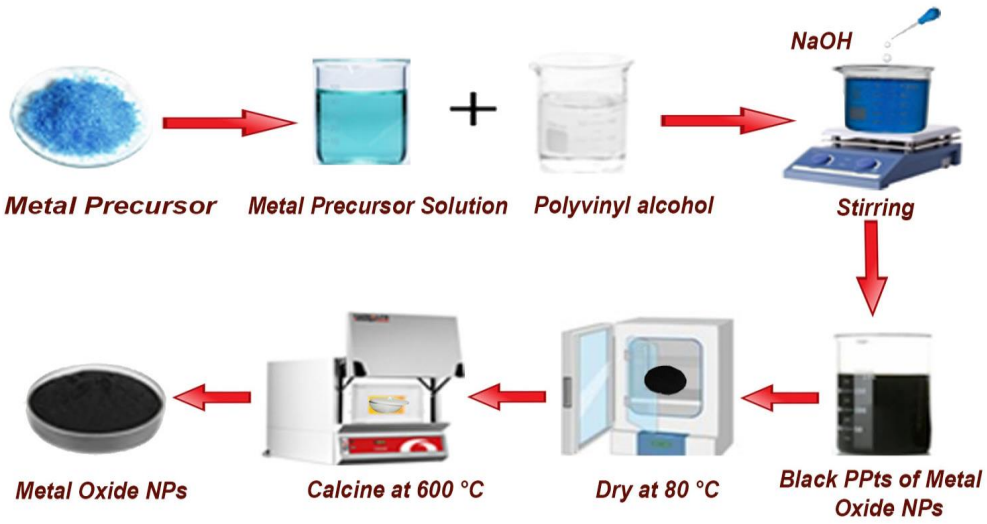

Fig. 2: Synthesis of metal oxide nanoparticles by sol gel method.

a 5% PVA solution. The mixture was heated at 75 °C until the pH level reached 10.8, at which point a 0.9M NaOH solution was added in drop wise increments. The mixture was then stirred at 70 °C for 2 hours. Green precipitates were autoclave at 160 °C for five hours. After centrifuging and washing the precipitate with distilled water, the pH of the mixture was adjusted to 7. Using an air dried oven set to 80 °C for 24 hours, the Cu-Co NCs were dried [26]. Fig. 2 represent general scheme for the synthesis of metal oxide nanoparticles by co-precipitation method.

Ferric chloride ($FeCl_3.6H_2O$) and Cobalt Chloride ($CoCl_2.4H_2O$), both at a concentration of 0.1M, were dissolved in 100 ml of a 5% solution of PVA. As the mixture was heated at 75 °C until the pH level reached 10.8, a 0.9M NaOH solution was added in drop wise increments. The green precipitates were synthesized and kept in an autoclave at 160 °C for five hours. After centrifuging and washing the precipitate with distilled water, the pH of the mixture was adjusted to 7. The synthesized Cu-Co NCs were then dried in an oven for 24 hours at 80 °C [26].

Determination of DPPH Radical Scavenging Activity

The free radical scavenging activity was assessed using 1,1-diphenyl-2-picryl-hydrazil (DPPH) following the method described by Gulcin et al. [27]. In ethanol, a 0.3 mM DPPH solution was prepared. Each sample was placed in a 500 mL beaker with 95 mLof an ethanol-based DPPH solution, and the weight of these samples ranged between 6.25 and 5.00 mg. The mixture was spread out in a 96-well plate and allowed to stand at 37° C for 30 minutes. Using a microliter plate reader (Spectramax plus 384 Molecular Device, USA), the absorbance at 515 nm was measured to determine the percentage of radical scavenging activity in comparison to the methanol-treated control. DPPH is frequently employed, as illustrated in equation 1:

$$DPPH\ scavenging\ effect\ (\%) = (A_c - \frac{A_s}{A_c}) \times 100 \quad (1)$$

Where,
Ac = Absorbance of control (DMSO treated), As = Absorbance of sample

Urease assay and inhibition

The reaction mixtures containing 25 ml of an enzyme (Jack bean urease) solution and 55 ml of buffers containing 100 mM urea in the test compounds added at a concentration of 1.0 mM. The mixtures were then incubated in 96-well plates for 15 min at 30 °C. To assess the urea's activity, ammonia production was evaluated using the indo phenol method. Each well received 70 ml of alkali reagent (0.5 w/v NaOH and 0.1% active chloride NaCl) and 45 ml of phenol reagent (1% w/v phenol and 0.005% w/v sodium nitro prusside, respectively). After a 50-minutes time interval, the increase in absorbance at 630 nm was detected using a microplate reader. The results (change in absorbance per minute) were processed with Soft

Max Pro software. The pH of 8.2 was used for all the experimental runs. Thio urea was the most popular urease inhibitor used in the past. The inhibition percentages were calculated using the following equation 2:

$$100 - \left(\frac{OD_{testwell}}{OD_{control}}\right) \times 100 \quad (2)$$

Characterization Techniques of Nanoparticles

The synthesized PEG coated nanoparticles were characterized by X-ray diffractometer (XRD, X'Pert PRO PAN analytical diffractometer, The Netherlands) with Cu Kα radiation (λ = 0.15406 nm). The SEM (FEI Quanta 250, Czech Republic) and Fourier Transform Infrared (FTIR) spectrophotometer (Thermo-Nicolet380, Warm Fisher, Madison, USA) were employed.

RESULTS AND DISCUSSION

Characterization of Nanocomposites:

The synthesized CuO NPs and Cu-Co, Cu-Mn nanocomposite were characterized by the rious techniques.

FTIR Spectra of Nanocomposites

Fourier transform infrared (FTIR) spectroscopy was used to analyze the chemical interactions between the PVA and CuO NPs. At 3392.79cm^{-1}, PVA's main feature reached its maximum value (O-H stretching) due to the presence of hydrogen bonding. 1402.25 cm^{-1} (C-H bending), 2900.00 cm^{-1} (C-H stretch vibration), 1625.99 cm^{-1} (C-O bending), 1200.22 cm^{-1} (C-O vibration), 1097.50 cm^{-1} (C-O stretching), and 1018.41 cm^{-1} (C-H bending) are the lengths that are bent in one direction (C-C stretching). The presence of weak and broad band's at approximately 3392.79 cm^{-1}across all groups suggested that the OH groups are related. The FTIR spectra of the PVA/CuO nanocomposite, which showed a band about 621.08 cm^{-1}, in addition to other peaks associated with PVA due to CuO stretching, supported the existence of copper oxide nanoparticles [28]. The FTIR spectrum of CuO nanoparticles is shown in Fig. 3 (a).

Fig. 3 (b) shows the FTIR spectrum of Cu-Mn nanocomposites in the range of 4000-400cm^{-1}. Fig. 3 (b) showsthe FTIR spectrum of Cu-Mn nanocomposites in the range of 4000-400cm^{-1}. The PVA's functional group was confirmed by FTIR at 607.58 cm^{-1}, 1126.43 cm^{-1}, 1390.68 cm^{-1}, 1631.78 cm^{-1}, and 3423.65 cm^{-1} by recording the peaks. It was predicted that the coated sample would exhibit a peak at 607.58 cm^{-1}, which corresponds to the Cu-distinctive O's absorption band. Peaks at around 1390.68 cm^{-1} for C-H bending modes and 1126.43 cm^{-1} for C-O-C stretch were found [29]. Water absorption is evidenced by the bands at 3423.65 cm^{-1} and 1631.78 cm^{-1}, which are attributable to the O-H stretching and H-O-H bending modes of vibration, respectively.

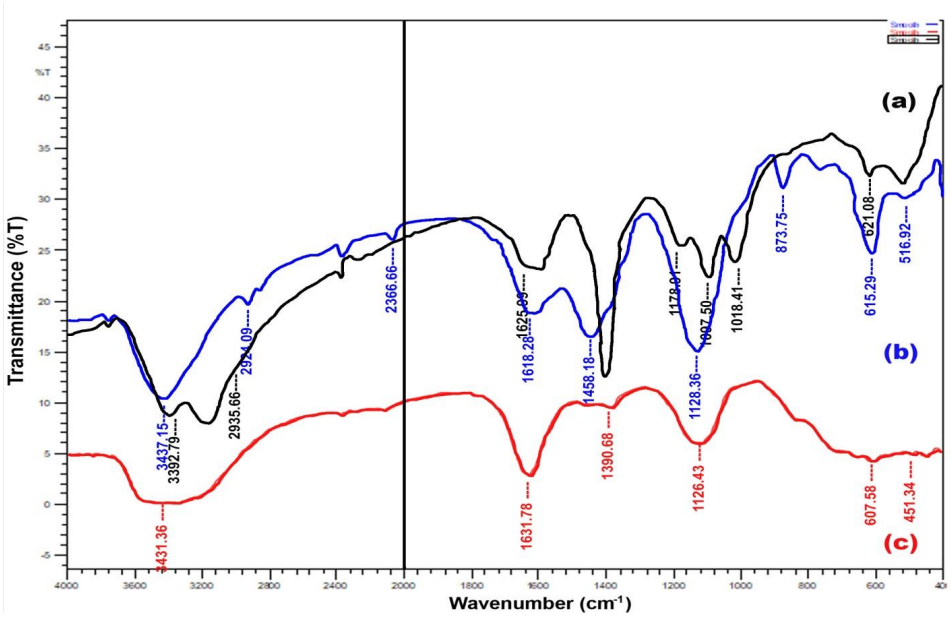

Fig. 3: FTIR images of (a) CuO-PVA NPs (b) Cu-Mn PVA NCs (c) Cu-Co PVA NCs at high resolution with scaling.

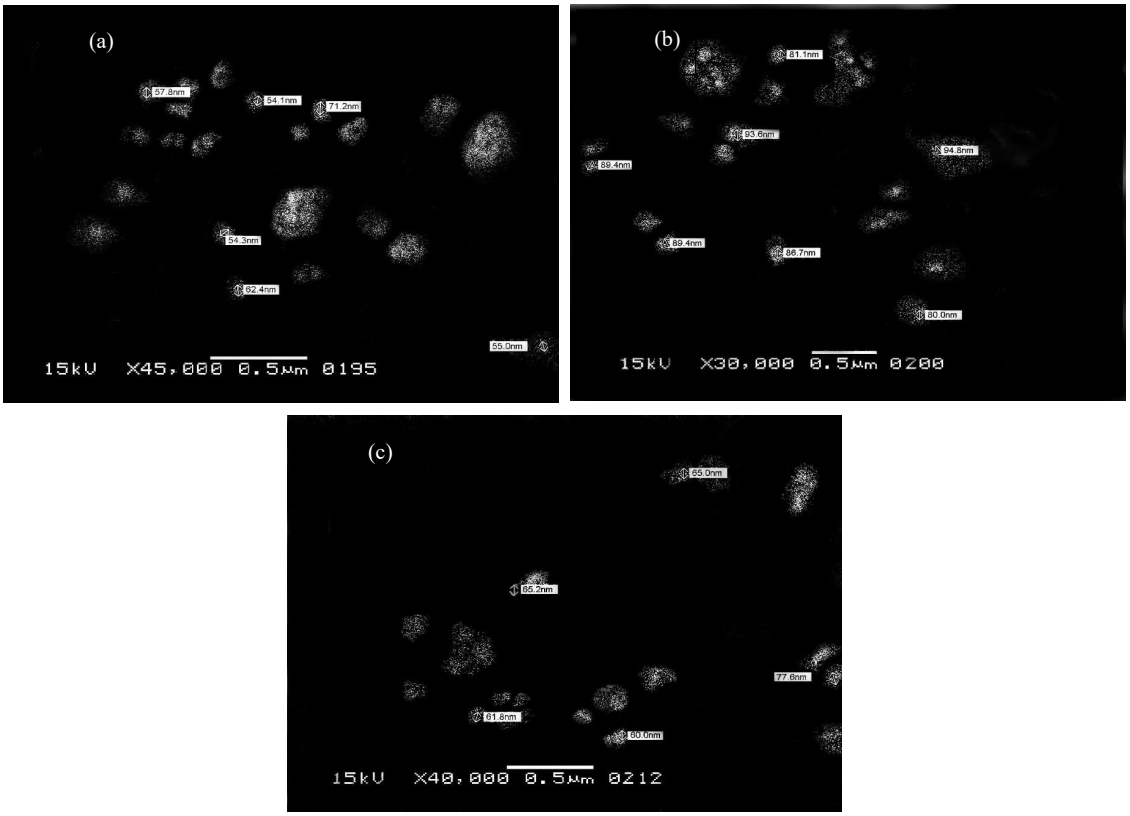

Fig. 4: SEM images of (a) CuOPVA NPs (b) Cu-Mn PVA NCs a (c) Cu-Co PVA NCs at high resolution with scaling.

The Cu-Co nanocomposite's FTIR spectra, was recorded to determine the presence of elements. A solid phase FTIR spectrum in the 400–4000 cm^{-1} region was obtained. The FTIR spectra of the sample verified the presence of the PVA coating on the Cu-Co NCs' surface. The signal at 615.29 cm^{-1} is predicted to prove the metallic composition of the produced nanoparticles. C-H bending modes and the C-O-C stretch are both observed at peaks around 1458.18 cm^{-1} and 1128.36 cm^{-1}, respectively. It is possible to explain the band at 1618.28 cm^{-1} by either hydrogen bonding between neighboring surfactants or by the presence of PVA oxidized species on the surface of the NPs. The adsorbed water-OH stretching mode was visible at 3437.15cm^{-1}[30]. Fig. 3 (c) depicts the Cu-Co NCs' FTIR spectrum.

Scanning Electron Microscopy of Nanocomposite

SEM analysis was done on the PVA-CuO surface characteristics. With an average size of 54.1–71.2 nm, pure PVA–CuO nanoparticles are shown in Fig. 4(a). The pure PVA patch exhibits morphologies that are constant, continuous, and bead-free. These consistent and streamlined morphologies formed a porous network that let nutrients and oxygen to permeate the connecting cells.

The PVA-CuO surface properties were examined by SEM. Fig. 4 (a) illustrates the pure PVA-CuO NPs with an average size of 54.1–71.2 nm. It shows uniform, continuous, and bead-free morphologies in the pure PVA patch. These consistent and streamlined morphologies formed a porous network that let nutrients and oxygen to permeate the connecting cells.

The Cu-Mn-surface PVA's properties were investigated by SEM images, as depicted in Fig. 4 (b). The size of the PVA-CuO NCs ranged from 80.0 to 94.8 nm. The images indicate that, in contrast to the Cu-Mn NC-loaded particles, the pure PVA patch exhibited uniform, continuous, and bead-free morphologies. These regular and slick morphologies produced a porous network that allowed nutrients and oxygen to diffuse the linked cells.

The SEM imageof Cu-Co-PVA nanocomposites is displayed in Fig. 4 (c). With the exception of somewhat bigger particle size and smoother

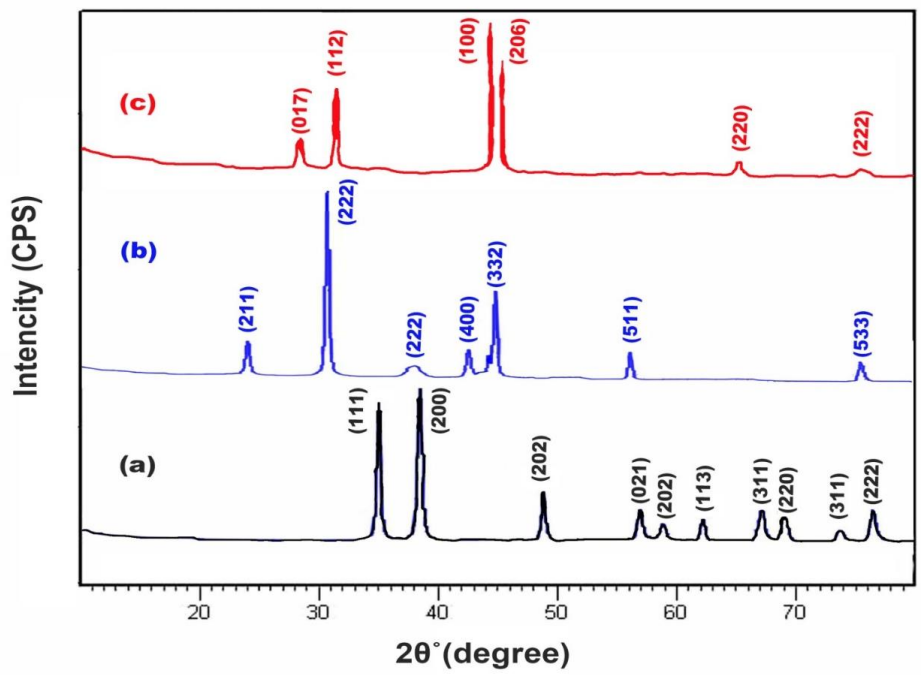

Fig. 5: XRD images of (a) CuO PVA NPs (b) Cu-Mn PVA NCs a and (c) Cu-Co PVA NCs at high resolution with scaling

Table 1: Antioxidant and Enzyme Inhibition Activities of Nanocomposites

Sr. #	Compound	Antioxidant Activity IC_{50} value (uM)	Urease Inhibition Activity IC_{50} value (uM)
1.	CuO NPs	78.9± 0.21	18.5± 056
2.	Cu-Mn NCs	67.8± 0.83	23.7± 0.71
3.	Cu-Co NCs	60.8± 0.76	34.5± 0.87
4.	BHA	44.2 ± 0.26	
5.	Thiourea	----------	21.5 ± 0.47

surface, the Cu-Co-PVA nanocomposites nevertheless have the morphological characteristics of CuO. PVA is uniformly coated on the surface of Cu-Fe nanocomposite to produce polymer shells. Cu-Co-PVA nanocomposites are spherical in shape and their sizes ranges from 60.0 nm to 77.6 nm.

X-ray Diffraction of Nanocomposites

The XRD diffraction patterns of CuO NPs' are shown in Fig. 5 (a). CuO NPs synthesized by the sol-gel method showed diffraction peaks at 2θ of 35.55, 38.73, 48.74, 56.56, 58.30, 61.56, 66.25, 68.13, 72.40, and 75.82. It indicates that it is in good accord with the reported values of the ICSD Card No. 087124 from the International Center for Diffraction Data. Using the Debye-Scherer formula, the synthesis of monoclinic CuO nanoparticles was evaluated and the average particle size was determined.

Fig. 5 (b) depicts the Cu-Mn NCs' XRD diffraction pattern. The diffraction peaks were observed at 2θ values of 23.14, 32.90, 38.26, 43.18, 45.06, 57.11, and 74.20. It was found to be in good agreement with the reported values of the ICSD Card No. 024106 from the International Center for Diffraction Data. Using the Debye-Scherer formula, the synthesized cubic Cu-Mn nanocomposites and their average particle size were assessed. The measured values ranged from 2 to 6 nanometers.

The powder X-ray diffraction method was applied to synthesize Cu-Fe NCs. By employing the appropriate lattice constants, these NCs preserved the rhombohedral structure. The XRD patterns and diffraction peaks used to confirm the crystalline structure are shown in Fig. 5 (c).

Antioxidant and Enzyme Inhibition Activities of Nanocomposites

The antioxidant and urease inhibition activities of CuO NPs, Cu-Mn NCs, and Cu-Co NCs are illustrated in Table 1.

CONCLUSION

In the present study the sol-gel method was applied to synthesize CuO NPs, Cu-Mn NCs, and Cu-Co NC. Polyvinyl alcohol (PVA) was used as a stabilizing agent and a number of techniques were employed to characterize these metal oxide nanocomposites. Fourier transform infrared spectroscopy (FTIR) proved that the PVA was bonded to CuO NPs, Cu-Mn NCs, and Cu-Co NCs. SEM analysis revealed that the average particle sizes for CuO NPs, Cu-Mn NCs, and Cu-Co NCswere64.5, 87.5, and 69.0 nm, respectively. The XRD pattern also confirmed the formation of NPs. The antioxidant activity of the above-mentioned NCs was measured against 2, 2-diphenyl-1-picryl-hydrazyl (DPPH). The enzyme inhibition activity of CuO NPs, Cu-Mn NCs, and Cu-Co NCs were determined to be 18.5, 23.7, and 34.5 uM, respectively, using urease as a standard. The antioxidant activities of CuO NPs, Cu-Mn NCs, and Cu-Co NCs with IC50 values were found to be 78.9, 67.8, and 60.8. It shows that the synthesized nanocomposites have significant values of antioxidant activities. These nanocomposites were effective to reduce the antiaging process, in cardiovascular diseases, cancer, and other free radical reactive diseases.

CONFLICT OF INTEREST

Authors have no conflicts of interest regarding the submitted manuscript.

ACKNOWLEDGMENTS

The authors are thankful to the department of Chemistry for providing necessary laboratory facilities.

REFERENCES

1. Jamshidi-Kia F, Wibowo JP, Elachouri M, Masumi R, Salehifard-Jouneghani A, Abolhassanzadeh Z, et al. Battle between plants as antioxidants with free radicals in human body. Journal of Herbmed Pharmacology. 2020;9(3):191-9. https://doi.org/10.34172/jhp.2020.25
2. Kolen'ko YV, Garshev AV, Churagulov BR, Boujday S, Portes P, Colbeau-Justin C. Photocatalytic activity of sol-gel derived titania converted into nanocrystalline powders by supercritical drying. Journal of Photochemistry and Photobiology A: Chemistry. 2005;172(1):19-26. https://doi.org/10.1016/j.jphotochem.2004.11.004
3. Jeevanandam J, Barhoum A, Chan YS, Dufresne A, Danquah MK. Review on nanoparticles and nanostructured materials: history, sources, toxicity and regulations. Beilstein journal of nanotechnology. 2018;9:1050-74. https://doi.org/10.3762/bjnano.9.98
4. Tahir H, Saad M, Attala OA, El-Saoud WA, Attia KA, Jabeen S, et al. Sustainable Synthesis of Iron–Zinc Nanocomposites by Azadirachta indica Leaves Extract for RSM-Optimized Sono-Adsorptive Removal of Crystal Violet Dye. Materials. 2023; 16(3). https://doi.org/10.3390/ma16031023
5. Ambekar AA, Sivaperumal P, Kamala K, Kubal P, Prakash C. Effect of temperature changes on antioxidant enzymes and oxidative stress in gastropod Nerita oryzarum collected along India's first Tarapur Atomic Power Plant site. Environmental Research. 2023;216:114334. https://doi.org/10.1016/j.envres.2022.114334
6. Sorbiun M, Shayegan Mehr E, Ramazani A, Mashhadi Malekzadeh A. Biosynthesis of metallic nanoparticles using plant extracts and evaluation of their antibacterial properties. Nanochemistry Research. 2018;3(1):1-16.
7. Kruk J, Aboul-Enein HY. Reactive Oxygen and Nitrogen Species in Carcinogenesis: Implications of Oxidative Stress on the Progression and Development of Several Cancer Types. Mini reviews in medicinal chemistry. 2017;17(11):904-19. https://doi.org/10.2174/1389557517666170228115324
8. Kumar N, Kumbhat S. Essentials in nanoscience and nanotechnology: John Wiley & Sons; 2016. https://doi.org/10.1002/9781119096122
9. Leon L, Chung EJ, Rinaldi C. Chapter 1 - A brief history of nanotechnology and introduction to nanoparticles for biomedical applications. In: Chung EJ, Leon L, Rinaldi C, editors. Nanoparticles for Biomedical Applications: Elsevier; 2020. p. 1-4. https://doi.org/10.1016/B978-0-12-816662-8.00001-1
10. Liu J, Chakraborty S, Hosseinzadeh P, Yu Y, Tian S, Petrik I, et al. Metalloproteins Containing Cytochrome, Iron-Sulfur, or Copper Redox Centers. Chemical Reviews. 2014;114(8):4366-469. https://doi.org/10.1021/cr400479b
11. Lovejoy DB, Guillemin GJ. The Potential for Transition Metal-Mediated Neurodegeneration in Amyotrophic Lateral Sclerosis. 2014;6. https://doi.org/10.3389/fnagi.2014.00173
12. Lushchak VI, Storey KB. Oxidative stress concept updated: Definitions, classifications, and regulatory pathways implicated. EXCLI journal. 2021;20:956-67.
13. Krstajić Pajić MN, Stevanović SI, Radmilović VV, Gavrilović-Wohlmuther A, Zabinski P, Elezović NR, et al. Dispersion effect in formic acid oxidation on PtAu/C nanocatalyst prepared by water-in-oil microemulsion method. Applied Catalysis B: Environmental. 2019;243:585-93. https://doi.org/10.1016/j.apcatb.2018.10.064
14. Mohd Mutalip SS, Ab-Rahim S, Rajikin MH. Vitamin E as an Antioxidant in Female Reproductive Health. Antioxidants (Basel, Switzerland). 2018;7(2). https://doi.org/10.3390/antiox7020022
15. Munteanu IG, Apetrei C. Analytical Methods Used in Determining Antioxidant Activity: A Review. International Journal of Molecular Sciences [Internet]. 2021; 22(7). https://doi.org/10.3390/ijms22073380
16. Nanda S, Nanda A, Lohan S, Kaur R, Singh B. Chapter

3 - Nanocosmetics: performance enhancement and safety assurance. In: Grumezescu AM, editor. Nanobiomaterials in Galenic Formulations and Cosmetics: William Andrew Publishing; 2016. p. 47-67. https://doi.org/10.1016/B978-0-323-42868-2.00003-6
17. Nor Azman NH, Goon JA, Abdul Ghani SM, Hamid Z, Wan Ngah WZ. Comparing Palm Oil, Tocotrienol-Rich Fraction and α-Tocopherol Supplementation on the Antioxidant Levels of Older Adults. Antioxidants [Internet]. 2018; 7(6). https://doi.org/10.3390/antiox7060074
18. Patil RS, Kokate MR, Jambhale CL, Pawar SM, Han SH, Kolekar SS. One-pot synthesis of PVA-capped silver nanoparticles their characterization and biomedical application. Advances in Natural Sciences: Nanoscience and Nanotechnology. 2012;3(1):015013. https://doi.org/10.1088/2043-6262/3/1/015013
19. Aziz MA, Diab AS, Mohammed AA. Antioxidant categories and mode of action. 2019;2019(Antioxidants):3-22.
20. Chainy GBN, Paital B, Dandapat J. An Overview of Seasonal Changes in Oxidative Stress and Antioxidant Defence Parameters in Some Invertebrate and Vertebrate Species. Scientifica. 2016;2016:6126570. https://doi.org/10.1155/2016/6126570
21. Chen QY, DesMarais T, Costa M. Metals and Mechanisms of Carcinogenesis. Annual Review of Pharmacology and Toxicology. 2019;59(1):537-54. https://doi.org/10.1146/annurev-pharmtox-010818-021031
22. Gupta P, Lakes A, Dziubla T. Chapter One - A Free Radical Primer. In: Dziubla T, Butterfield DA, editors. Oxidative Stress and Biomaterials: Academic Press; 2016. p. 1-33. https://doi.org/10.1016/B978-0-12-803269-5.00001-2
23. Fardood ST, Moradnia F, Moradi S, Forootan R, Zare F, Heidari M, editors. Eco-friendly synthesis and characterization of α-Fe2O3 nanoparticles and study of their photocatalytic activity for degradation of Congo red dye2019.
24. Wongpisutpaisan N, Charoonsuk P, Vittayakorn N, Pecharapa W. Sonochemical Synthesis and Characterization of Copper Oxide Nanoparticles. Energy Procedia. 2011;9:404-9. https://doi.org/10.1016/j.egypro.2011.09.044
25. Xiao X, Zhang Z, Nan F, Zhao Y, Wang P, He F, et al. Mesoporous CuCo2O4 rods modified glassy carbon electrode as a novel non-enzymatic amperometric electrochemical sensors with high-sensitive ascorbic acid recognition. Journal of Alloys and Compounds. 2021;852:157045. https://doi.org/10.1016/j.jallcom.2020.157045
26. Yakushkin SS, Balaev DA, Dubrovskiy AA, Semenov SV, Knyazev YV, Bayukov OA, et al. ε-Fe2O3 nanoparticles embedded in silica xerogel - Magnetic metamaterial. Ceramics International. 2018;44(15):17852-7. https://doi.org/10.1016/j.ceramint.2018.06.254
27. Yan Z, Spaulding HR. Extracellular superoxide dismutase, a molecular transducer of health benefits of exercise. Redox Biology. 2020;32:101508. https://doi.org/10.1016/j.redox.2020.101508
28. Saad M, Tahir H, Mustafa S, Attala OA, El-Saoud WA, Attia KA, et al. Polyvinyl Alcohol Assisted Iron–Zinc Nanocomposite for Enhanced Optimized Rapid Removal of Malachite Green Dye. Nanomaterials [Internet]. 2023;13(11). https://doi.org/10.3390/nano13111747
29. Yusuf S, Bosch J, Dagenais G, Zhu J, Xavier D, Liu L, et al. Cholesterol Lowering in Intermediate-Risk Persons without Cardiovascular Disease. New England Journal of Medicine. 2016;374(21):2021-31. https://doi.org/10.1056/NEJMoa1600176
30. Taghavi Fardood S, Moradnia F, Heidarzadeh S, Naghipour A. Green synthesis, characterization, photocatalytic and antibacterial activities of copper oxide nanoparticles of copper oxide nanoparticles. Nanochemistry Research. 2023;8(2):134-40.